



Design of Broadband Matching Network for Complex Reactive Load using L-Matching

Jawad Yousaf*, Zubair Mehmood, Waseem Abbas, and Khuram Shehzad

Department of Electrical and Electronics Engineering,
Sungkyunkwan University, Suwon, Republic of Korea

Abstract: In this work, effect of single and multisection matching with and without ideal lumped components on the impedance matching bandwidth was analyzed. Single and multisection L-matching networks are designed for parallel reactive (RC) load configuration at 10 GHz. The analysis showed that higher section matching with ideal components did not produce significant improvement in fractional bandwidth of matching network for complex parallel RC load. However, more wider impedance bandwidth can be obtained with lower section matching constituting of finite component quality factor (Q) lumped components.

Keywords: L-matching, broadband impedance matching, ideal/non-ideal lumped matching

1. INTRODUCTION

Matching networks are designed to ensure the maximum power transfer between the transmitter and receiver at the desired frequency range [1]. The maximization of the power transfer reduces the input reflection which is essential at every interface of the complete RF network for the achievement of higher overall efficiency of network. Both kinds of short and broadband conjugate matching network are designed depending on the requirements of the RF product or system [2, 3]. Besides the maximum power transfer, impedance matching is done to minimize the noise figure in low noise amplifier (LNA), achievement of maximum saturated output power for the power amplifiers (PA) and minimization of the ripples in the gain response of transmission line terminations [2 - 6]. Also the commercial ports of all RF products are designed with 50Ω source and load impedance which also invokes the needs of impedance matching [7, 8]. Fig. 1 illustrate the typical source and load side impedance matching networks. Matching bandwidth is defined as the range for which the input reflection i.e. S_{11} is lower than the threshold or the transfer characteristics, i.e., S_{21} are higher than the threshold.

The typical values of S_{11} and S_{21} threshold are -10 dB -3 dB respectively [1]. The matching network which has around 10 % fractional bandwidth is termed as narrow-band matching network, while the network with more than 30 % fractional bandwidth is known as broadband matching network [9]. L-matching, T-matching and single stub transmission line matching networks are common choices for the narrow band matching. For the broadband matching, multisection L/T matching, multisection quarter-wave transformer and tapered line matching are recommended [7, 8]. The lossless or low loss matching (with components having high quality factor Q like capacitors, inductors, transmission lines and transformers) have no or minimal power loss, and is usually results in narrow band matching [3-6]. The usage of lossy components having finite Q have power losses increase the power losses. However finite Q value increase the insertion loss which results in broadband matching.

In this work, we are presenting an analysis of the effect of single and multisection matching network with ideal and non-ideal passive components on the matching bandwidth. The single and multisection L-matching network are designed for the parallel RC load impedance using the step-down transformation. Non-ideal components are modeled by using finite Q characteristics of those components in circuit simulator. Advanced design system [10] is used for the simulation of all matching circuits. Fractional bandwidth is calculated and compared for all matching strategies. Details of the matching network design strategy and analysis of results for ideal and lossy components are elaborated in the following sections.

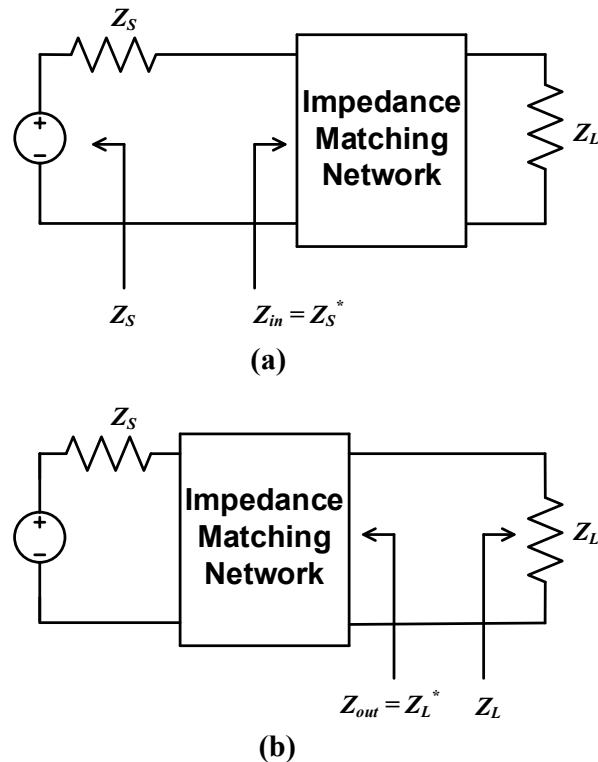


Fig. 1. Impedance matching network: (a) Source side matching; (b) Load-side matching.

2. LOAD CONFIGURATION

The analysis is performed for the a complex load impedance configuration constituting of resistive and capacitive components. The purpose is to the evaluate the effect of different matching strategies for the prototype load. Fig. 2 shows the load configuration. The load impedance contains a parallel network of resistor ($R=200 \Omega$) and capacitor ($C=1.2 pF$). This complex load impedance (Z_L) needs to be matched with standard 50Ω source impedance (Z_S).

3. L-MATCHING

L-matching is categorized into two classes: step-up and step-down transformation. Fig. 3 depicts the difference between these two classes. Step-up transformation is done when the source impedance is higher than the load impedance. For the case where load impedance is higher than source impedance, step down transformation is applied. The main difference occurs in the calculations of the transformation ratio (m) and transformation quality factor (Q) depending on the type of the selected transformation. Fig. 2 in our case, is the step down transformation scenario.

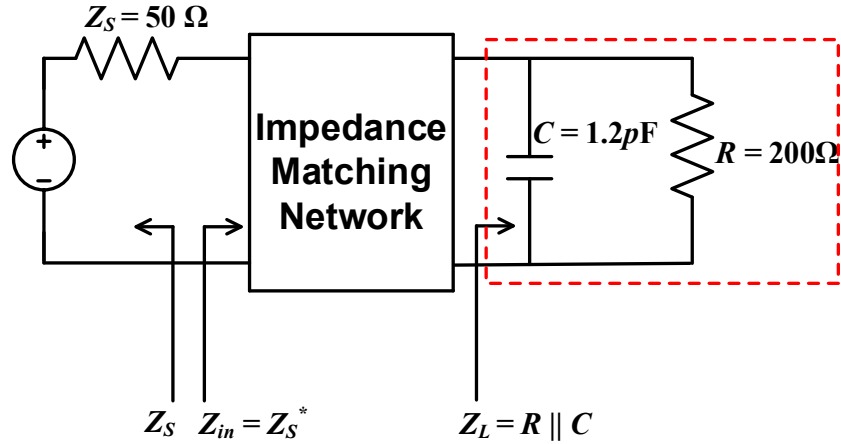


Fig. 2. Load impedance details.

The value of m and Q for a single section L-matching are computed using the Eq. 1. The computation of matching network components is dependent on the calculated values of m and Q .

$$m = \frac{R_S}{R_L} \rightarrow \text{for step - up}$$

$$m = \frac{R_L}{R_S} \rightarrow \text{for step - down} \quad (1)$$

$$Q = (m - 1)^{\frac{1}{2}}$$

For a multisection step-down transformation scenario as shown in Fig. 4.

The overall transformation ratio (m), overall transformation Q , per-stage ratio of transformation (m_i) and per-stage transformation (Q_i) can be computed as follows [1]:

$$\text{Overall Transformation Ratio: } m = \frac{R_L}{R_S} = m_i^N$$

$$\text{Overall Transformation - } Q: Q = (m - 1)^{\frac{1}{2}}$$

$$\text{Per - Stage Transformation Ratio: } m_i = \left(\frac{R_L}{R_S}\right)^{\frac{1}{N}} \quad (2)$$

$$m_i = \frac{R_L}{R_{i1}} = \frac{R_{i1}}{R_{i2}} = \frac{R_{i2}}{R_{i3}}, \dots, = \frac{R_{i(N-1)}}{R_{iN}}$$

$$\text{Per - Stage Transformation - } Q: Q_i = (m_i - 1)^{\frac{1}{2}}$$

For a step-up transformation, the position of the R_L and R_S can be exchanged in the above design steps.

4. MATCHING STRATEGY WITH IDEAL COMPONENTS

The impedance matching network for the load impedance of Fig. 2 are designed using step-down L-matching technique. Three kinds of matching network: single section, double section and triple section are designed. It should be noted that the complex load impedance needs to be converted to pure resistive impedance for the start of the impedance matching process using L section matching. For the complex load of Fig. 2, a shunt inductive component has to be added across the capacitive components to cancel the effect of complex components of load impedance.

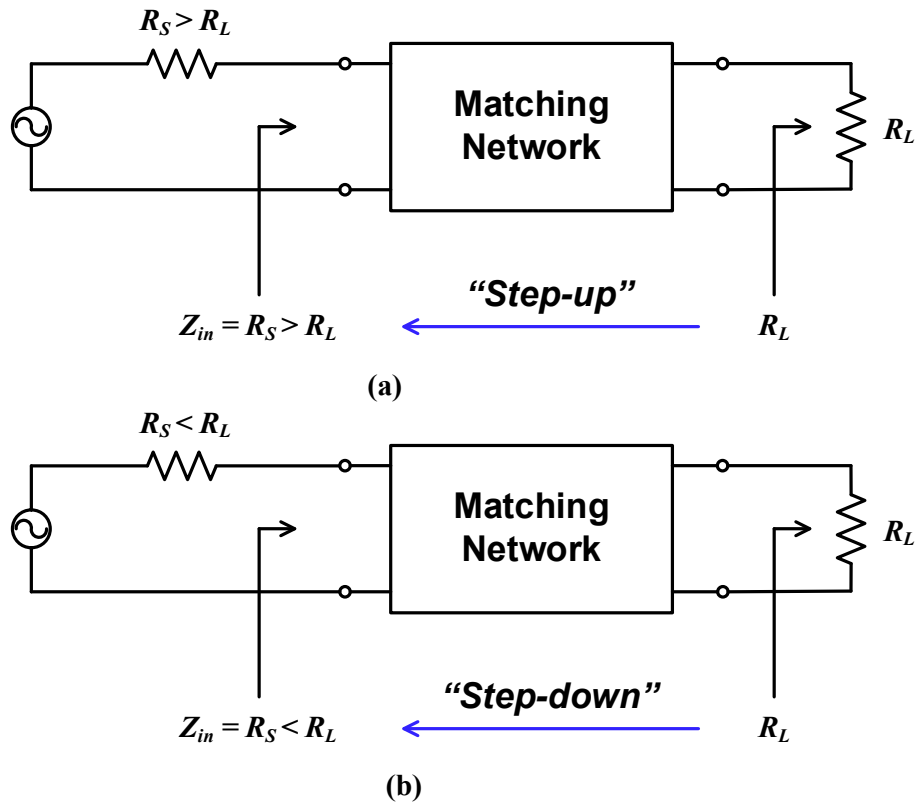


Fig. 3. L-matching configurations (a) Step-up transformation (b) Step-down transformation.

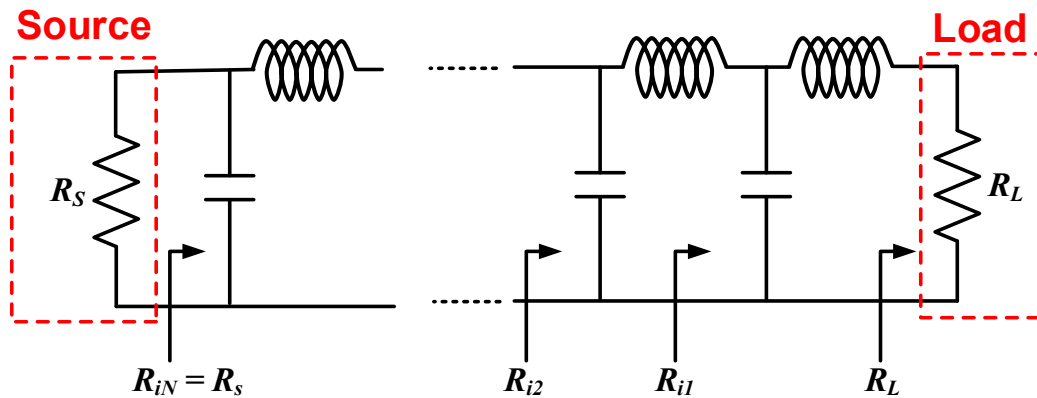


Fig. 4. Multisection L-matching configuration for step-down transformation ($R_S < R_L$).

The value of the shunt inductive element is calculated to make the complex part of the load impedance to zero. The value of L_{shunt} can be computed using the Eq. 3 at design frequency $f = 10 \text{ GHz}$. The adding of L_{shunt} makes the load impedance pure resistive i.e $Z_L = R_L = 200\Omega$. The values of this shunt inductive component can be combined with the final matching components of impedance matching network.

$$L_{shunt} = \frac{1}{\omega^2 C} = 0.211nH ; \omega = 2 \pi f \tag{3}$$

The comparison of the fractional bandwidth for each case is illustrated in the following subsections.

4.1 Single Section L-matching

The design steps for the single section L -matching with $R_L = 200 \Omega$ and $R_S = 50 \Omega$ based on Eq. 2 are given below.

$$m = \frac{R_L}{R_S} = 4$$

$$Q = (m - 1)^{\frac{1}{2}} = 1.73$$

$$X_{L1} = \frac{R_L}{Q} = 115.47 \Omega$$

$$L_1 = \frac{X_{L1}}{\omega} = 1.83 \text{ nH}$$

$$X_{C1} = Q \times R_S = 86.5 \Omega$$

$$C_1 = \frac{1}{\omega C} = 0.183 \text{ pF}$$

For the single section matching, the value of combined inductance of matching network is 0.189 nH . Table 1 depicts the all parameters of the single section L -matching. The designed matching network is simulated in ADS and its schematic is shown in Fig. 5. As depicted from the smith chart result [Fig. 6], the network is perfectly matched with the 50Ω source load. The simulated S -parameters of the designed single section matching network are shown in Fig. 7. The fractional bandwidth of the matching network is computed using the formula of Eq. 4. For the single section matching network, the fractional bandwidth is 4.04 % which can be computed from Fig. 7.

$$\text{Fractional Bandwidth} = \frac{f_{\text{high|limit}} - f_{\text{low|limit}}}{f_r} \% ; \text{ Where limit} = S_{11} \leq -10\text{dB} \quad (4)$$

Table 1. Single section L-matching parameters.

	1st Section
m	4
Q	1.73
$L_{\text{shunt}} \text{ (nH)}$	0.211
$X_L \text{ (}\Omega\text{)}$	115.4
$L \text{ (nH)}$	1.83
$X_C \text{ (}\Omega\text{)}$	86.5
$C \text{ (pf)}$	0.183
$Z_{\text{in}} \text{ (}\Omega\text{)}$	50.0

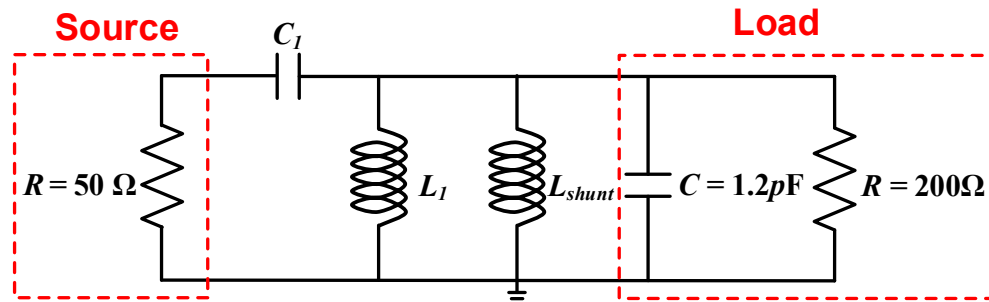


Fig. 5. Single section matching network (see Table 1 for Component values).

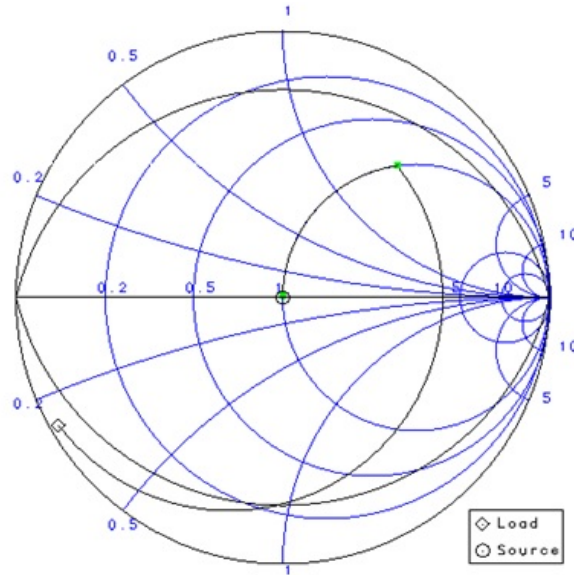


Fig. 6. Smith chart results of single section matching network.

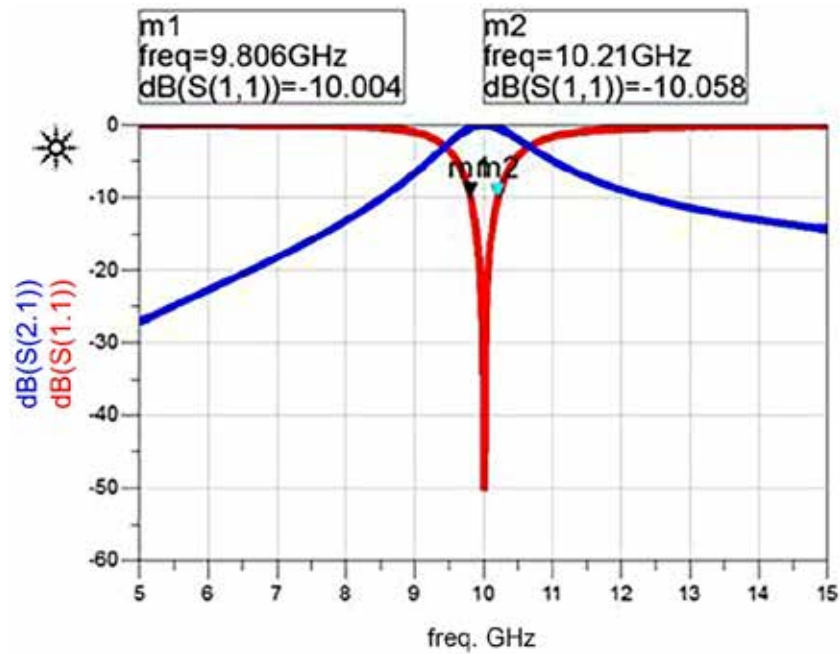


Fig. 7. S-parameter results of single section matching network.

4.2 Double Section L-matching

The parameters of the designed dual section *L*-matching network are computed using Eq. 2 and are shown in Table 2. The matching network is designed using the calculated parameters of Table 2 and its ADS schematic is shown in Fig. 8. Smith chart and scattering parameters of the matching network are shown in Fig. 9 and 10, respectively. The simulated fractional bandwidth in this case [Fig. 10] is 4.15 %.

Table 2. Double section L-matching parameters.

	1st Section	2nd Section
m	2	2
Q	1	1
$L_{shunt} (nH)$	0.211	
$X_L (\Omega)$	200	100
$L (nH)$	3.18	1.59
$X_C (\Omega)$	100	50
$C (pf)$	0.159	0.318
$Z_{in} (\Omega)$	150	50.0

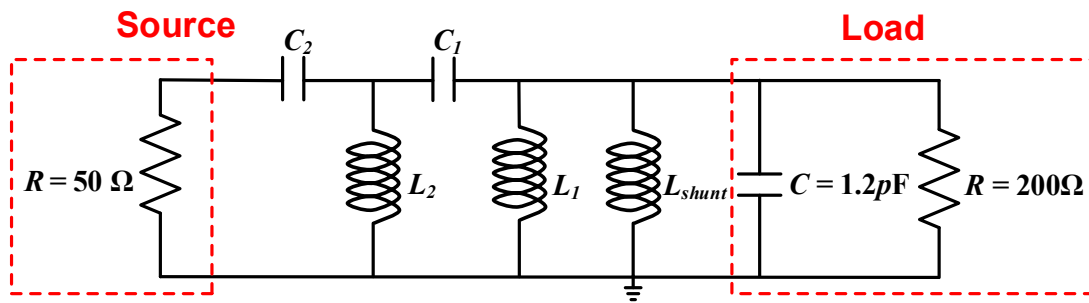


Fig. 8. Double section matching network (see Table 2 for Component values).

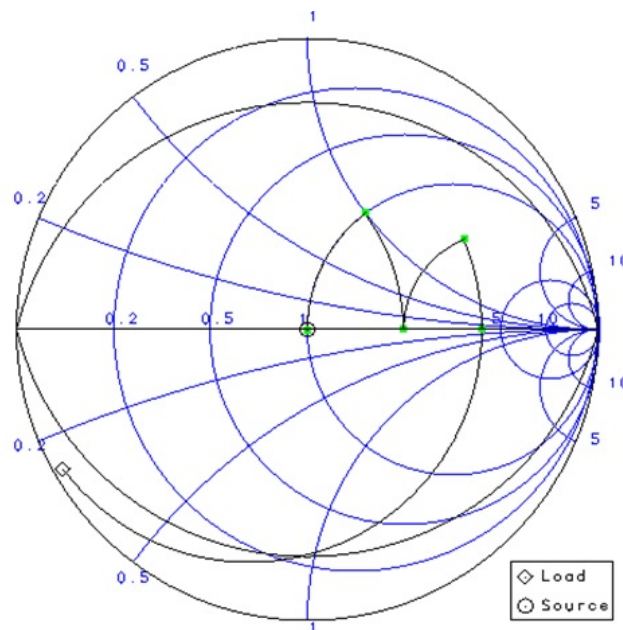


Fig. 9. Smith chart results of double section matching network.

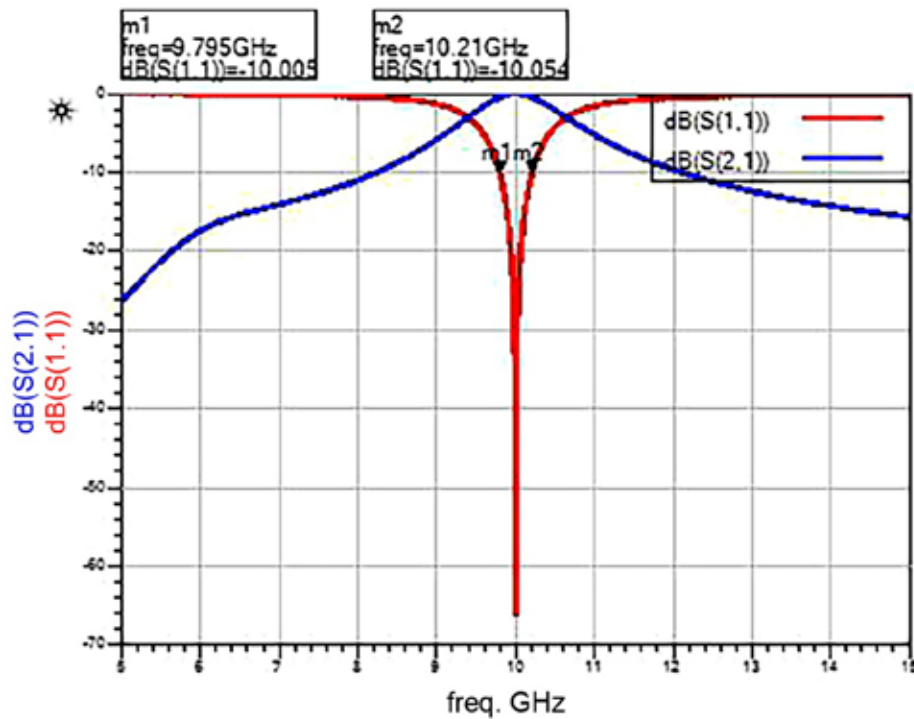


Fig. 10. S-parameter results of double section matching network.

4.3 Triple Section L-matching

The triple section matching network constitutes of three individual networks of L and C . Table 3 illustrate the parameters values for this scenario which can be computed using Eq. 2. Fig. 11 depicts the circuit diagram of the triple section L -matching network with source and load. Scattering parameter results for this case are shown in Fig. 13. It can be noted from Fig. 13 that triple section matching network exhibit only 4.21 % which is slight higher than single and double section matching networks but still is quite low.

Table 3. Triple section L-matching parameters.

	1st Section	2nd Section	Third Section
m	1.58	1.58	1.58
Q	0.76	0.76	0.76
$L_{shunt} (nH)$		0.211	
$X_L (\Omega)$	260.95	164.39	103.55
$L (nH)$	4.153	2.616	1.648
$X_C (\Omega)$	95.56	60.83	38.32
$C (pf)$	0.1648	0.2616	0.415
$Z_{in} (\Omega)$	125.9	79.37	50.0

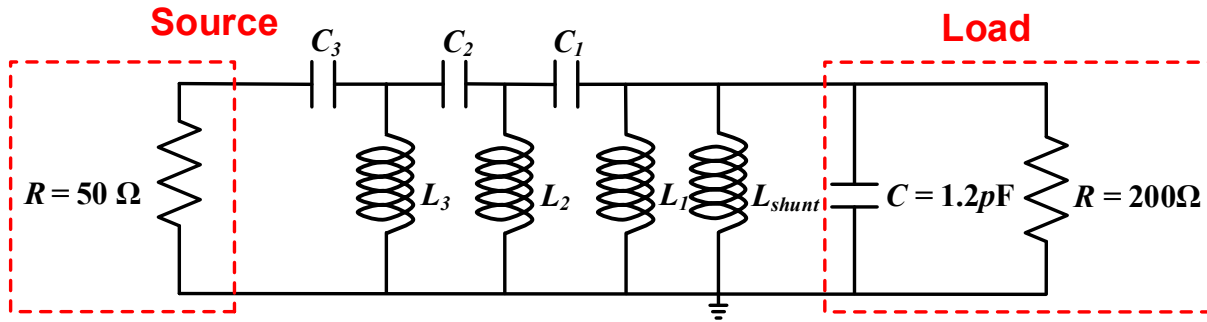


Fig. 11. Triple section matching network (see Table 3 for Component values).

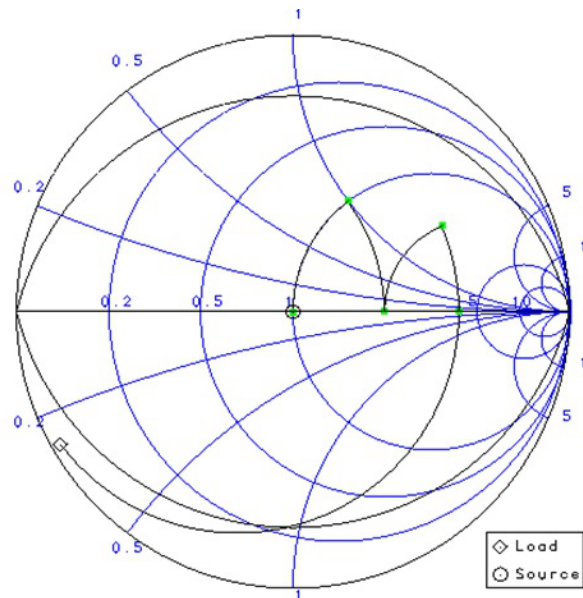


Fig. 12. Smith chart results of triple section matching network.

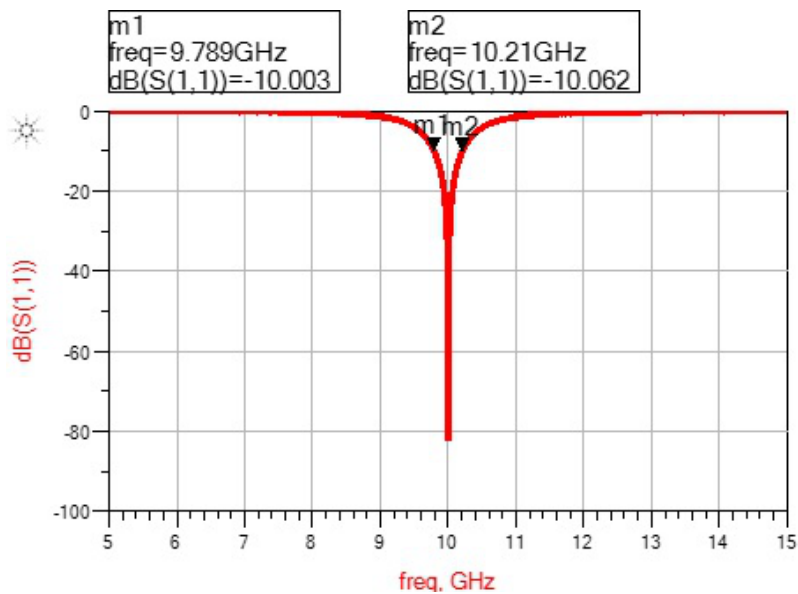


Fig. 13. S-parameter results of triple section matching network.

4.4 Four Section L-matching

The designed parameter for the four section matching are shown in Table 4. ADS schematic of the four section *L*-matching network is depicted in Fig. 14. Fig. 15 and Fig.16 show the simulated smith chart and *S*-parameters results of the the designed matching network respectively. The computed fractional bandwidth of this higher section matching network (4.35 %) is still lower than even 10 % of the narrow-band matching network limit.

Table 4. Fourth section L-matching parameters.

	1st Section	2nd Section	Third Section	Fourth Section
<i>m</i>	1.41	1.41	1.41	1.41
<i>Q</i>	0.64	0.64	0.64	0.64
<i>L_{shunt}</i> (nH)			0.211	
<i>X_L</i> (Ω)	310.7	219.73	155.37	109.86
<i>L</i> (nH)	4.958	3.497	2.472	1.748
<i>X_C</i> (Ω)	91.018	64.359	45.509	32.179
<i>C</i> (pf)	0.174	0.247	0.349	0.494
<i>Z_{in}</i> (Ω)	141.42	100.0	70.71	50.0

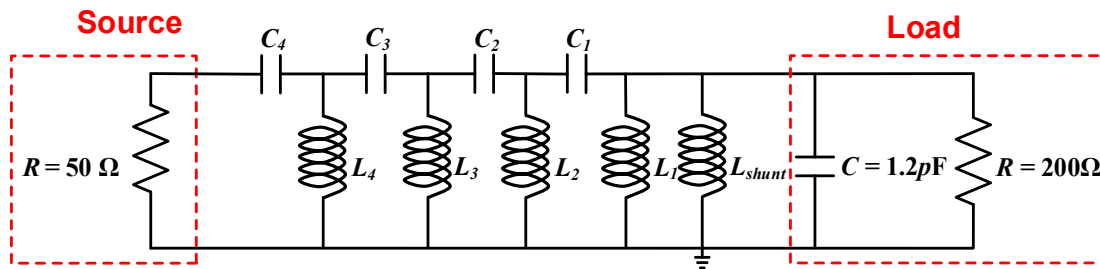


Fig. 14. Fourth section matching network (see Table 4 for Component values).

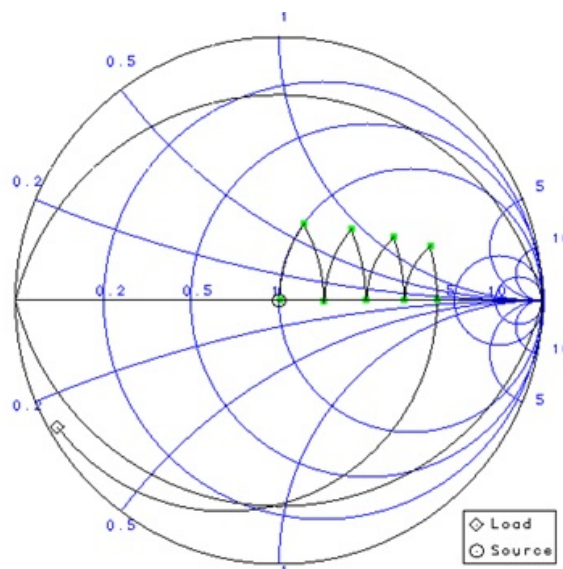


Fig. 15. Smith chart results of fourth section matching network.

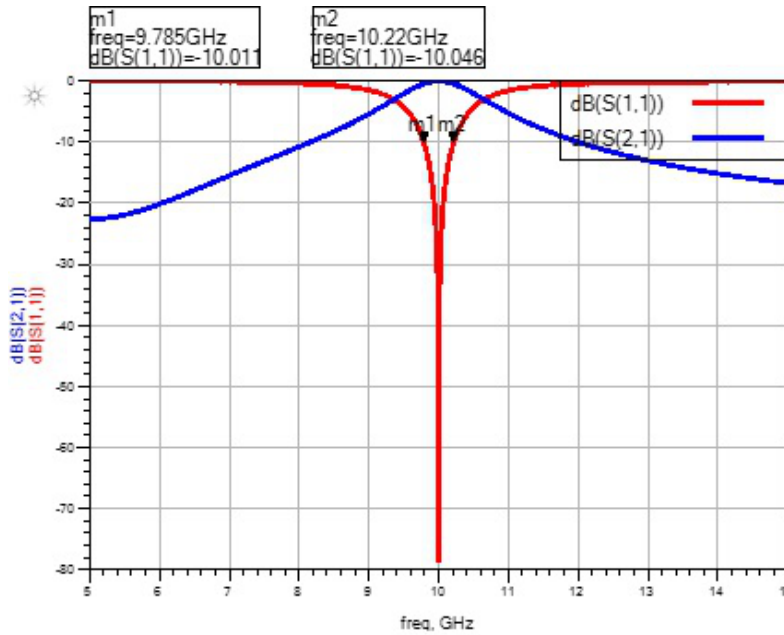


Fig. 16. S-parameter results of fourth section matching network.

4.5 Comparison of Results

The comparison of the fractional bandwidth for all four cases of single, double, triple and four section *L*-matching network is shown in Fig. 17. The results of Fig. 17 depicts that even the increase in number of matching section did not produce any significant improvement in the fractional bandwidth. The fractional bandwidth improvement difference is also not very high with the increase in matching network from three to four section. It shows that higher fractional bandwidth of more than 10 % or 30 % cannot be achieved with the ideal lumped components used for the all cases of single and multisection matching networks. For the achievement of broadband matching, the non-ideal components are good choice. The details of the enhancement in the matching bandwidth with non-ideal lumped components is elaborated in next section.

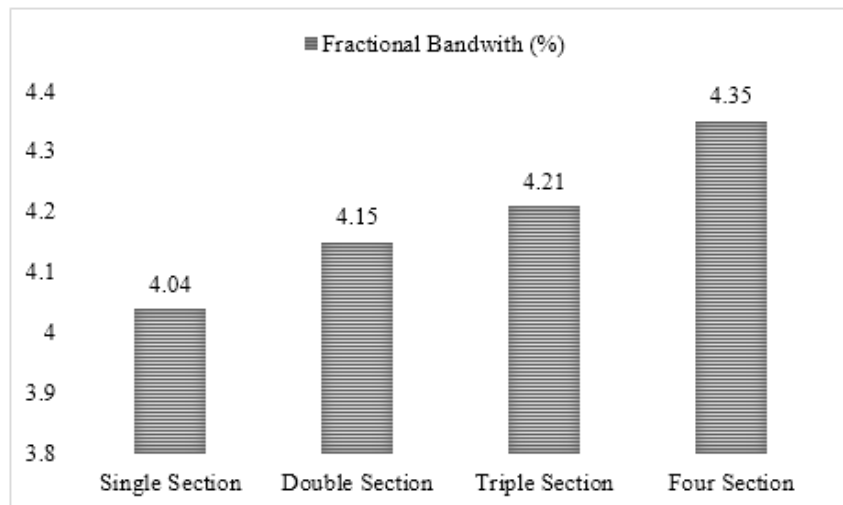


Fig. 17. Comparison of single and multisection *L*-matching with ideal *L/C*.

5. MATCHING STRATEGY WITH NON-IDEAL COMPONENTS

The fractional bandwidth can be increased by using lossy L and C components. The lossy L/C are modeled using finite Q value in the circuit simulation environment of ADS. The selected individual Q value for the lossy components is 2. The value of 2 is chosen after the turning of the matching network for good results. The schematic of the matching network with finite Q for triple section matching network is similar to shown in Fig. 11 with same component values as shown in Table 3 with the finite Q values. Fig. 18 reflects the comparison of the increase in the fractional bandwidth with the lossy L/C . Fig. 18 shows that fractional bandwidth for the three-section L -matching network with finite Q is 62.8 %. The lower section matching did not produce good results for the fractional bandwidth with the finite Q values.

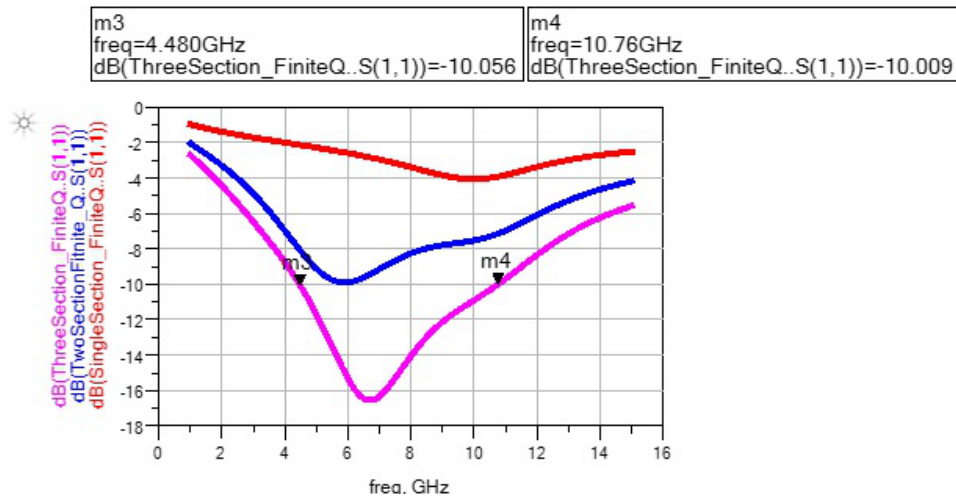


Fig. 18. Comparison of multisection L -matching with finite component Q .

6 COMPARISON OF IDEAL AND LOSSY MATCHING

The comparison of the fractional bandwidth of the matching network with lossy and ideal components is discussed in this section. Fig. 19 depicts the differences between the fractional bandwidth with ideal and lossy components having finite Q . It shows that significant improvement in fractional bandwidth (around 60 %) is observed for the three section L -matching network with ideal (infinite component Q) and lossy components (finite component Q). This increase in bandwidth is due to the reduction in the insertion loss of the matching network with finite component Q .

The insertion loss for the multisection L -matching network can be written as in Eq. 5 [1]. The adding of additional sections lower the Q values which eventually reduces the insertion loss. However the optimum number of matching network has to be chosen as the adding of too many matching networks can counterbalance the benefit of lowering of the insertion loss and consequentially improvement in the fractional bandwidth of the matching network [1, 2, 6].

$$Insertion\ Loss\ (IL) \equiv \frac{P_L}{P_{in}} = \left(\frac{1}{1 + \frac{Q_i}{Q_c}} \right)^{2N} \quad (5)$$

$$IL \cong \frac{1}{1 + 2N \left(\frac{Q_i}{Q_c} \right)}$$

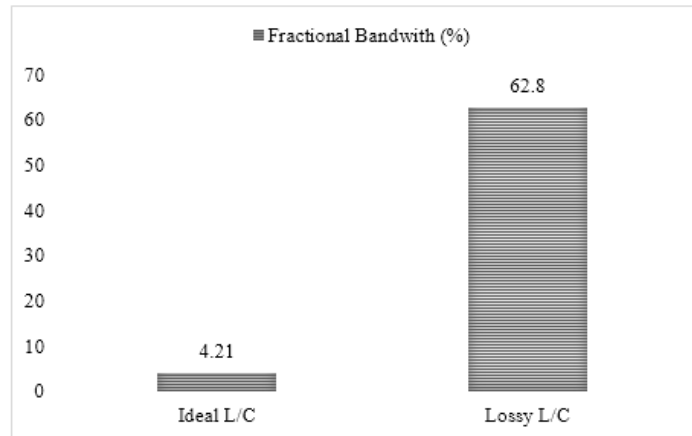


Fig. 19. Comparison of three-section L-matching with Finite and Infinite Q .

7 CONCLUSIONS

This study has presented an in-depth analysis of effect of ideal and lossy components on bandwidth of the matching network using L-matching. The ideal components produces very low fractional bandwidth even with four-section L-matching, for a complex load of $200 \Omega || 1.2 pF$. The three-section L-matching with finite component Q value of 2 produces the 62.8 % fractional bandwidth. The lowering of quality factor of individual components of the matching network reduces the insertion loss values and, hence, results in a wider bandwidth of the matching circuit. The presented design of three-section L-matching with finite Q value produces approximately 63 % matching bandwidth for $S_{11} \leq -10$ dB.

8. ACKNOWLEDGMENTS

We would like to thank Mr. Zaffar Hayat Nawaz Khan for his interactive discussions on impedance matching.

9. REFERENCES

1. Amin, M., J. Yousaf, & S. Iqbal. Single feed circularly polarised omnidirectional bifilar helix antennas with wide axial ratio beamwidth. *IET Microwaves, Antennas Propagation* 10: 825–830 (2013).
2. Chen, L-Y V., R. Forse, D. Chase, & R.A. York. Analog tunable matching network using integrated thin-film bst capacitors. In: *Proceedings Microwave Symposium Digest, 2004 IEEE MTT-S International*, p. 261–264 (2004).
3. Oraizi, H. & A-R Sharifi. Design and optimization of broadband asymmetrical multisection wilkinson power divider. *IEEE Transactions on Microwave Theory and Techniques* 54: 2220–2231 (2006).
4. Pozar, D. *Microwave Engineering*. John Wiley & Sons, NJ, USA (2009).
5. Vendelin, G.D., A.M. Pavio, & U.L. Rohde. *Microwave Circuit Design using Linear and Nonlinear Techniques*. John Wiley & Sons, NJ, USA (2005).
6. Yang, Y., J. Yi, Y.Y. Woo, & B. Kim. Optimum design for linearity and efficiency of a microwave doherty amplifier using a new load matching technique. *Microwave Journal* 44: 20-36 (2001).
7. Yousaf, J., H. Jung, K. Kim, & W. Nah. Design, analysis, and equivalent circuit modeling of dual band pifa using a stub for performance enhancement. *Journal of Electromagnetic Engineering and Science* 16: 169–181 (2016).
8. Yousaf, J., M. Amin, S. Iqbal, & H. Durrani. Analysis of conducted emission measurements of dc-dc converter with load for proper filter design. *International Journal of Microwave and Optical Technology* 10: 464–470 (2015).
9. Yousaf, J., M. Amin, & S. Iqbal. Circularly polarized wide axial ratio beamwidth omnidirectional bifilar helix antennas. In: *Proceedings IEEE First AESS European Conference on Satellite Telecommunications (ESTEL)*, p. 1–6 (2012).
10. *Advanced Design System (ADS)*. KEYSIGHT Technologies (2017) <http://literature.cdn.keysight.com/litweb/pdf/5988-3326EN.pdf?id=921864>.